Supplement of Atmos. Chem. Phys., 23, 5119–5133, 2023
https://doi.org/10.5194/acp-23-5119-2023-supplement

Atmospheric Chemistry and Physics
Open Access

Supplement of

Insights into characteristics and formation mechanisms of secondary organic aerosols in the Guangzhou urban area

Miaomiao Zhai et al.

Correspondence to: Ye Kuang (kuangye@jnu.edu.cn) and Li Liu (liul@gd121.cn)

1. Aerosol liquid water concentration calculation

The size resolved aerosol liquid water content (ALWC) was formulated as the following in which the ALWC was the summation of aerosol water contributed by inorganic aerosols and organic aerosols:

$$ALWC=ALWC_{Inorg} + ALWC_{LOOA}+ ALWC_{MOOA}$$

Where the $ALWC_{Inorg}$ was calculated using the ISORROPIA (Kuang et al., 2018) model using reverse mode and metastable with size resolved inorganic aerosol chemical compositions measured by the Q-ACSM as inputs. The SOA factors LOOA and MOOA are treated as hydrophilic components whereas POA factors HOA and COA are treated as hydrophobic components as discussed in Liu et al. (2022). Using the derived κ_{LOOA} and κ_{MOOA} of 0.13 and 0.23 in Liu et al. (2022) due to their similar O/C values, $ALWC_{LOOA}$ and $ALWC_{MOOA}$ was calculated as the following by assuming densities of LOOA and MOOA as 1.2 and 1.4 g/cm^3 following Liu et al. (2022):

$$ALWC_{SOA}=\frac{m_{SOA}}{\rho_{SOA}} \times \rho_w \times \frac{\kappa_{SOA}}{(\frac{100\%}{RH}-1)}$$

The m_{SOA} is the mass concentrations of SOA factors.

2. Supplement Figures for Source Apportionments

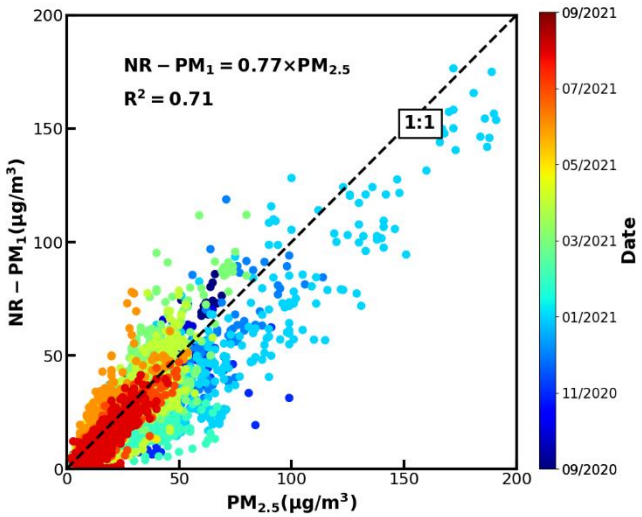

Figure S1. Correlation between NR-PM_1 and $PM_{2.5}$ for the entire year.

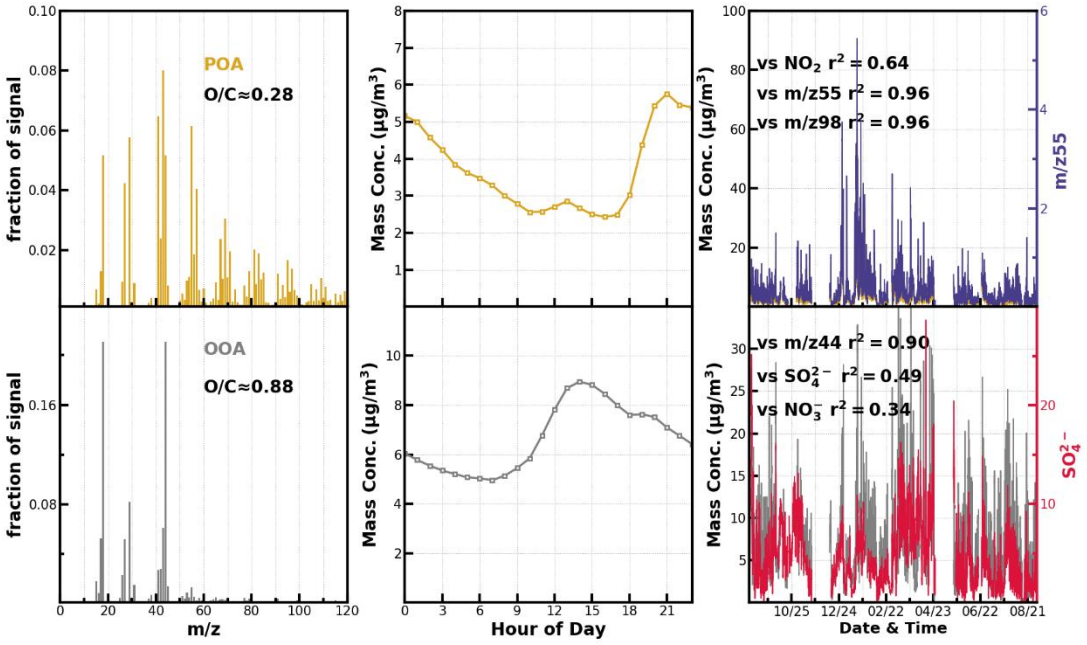

Figure S2. Results from the 2-factor solution of PMF-ACSM for the entire dataset.

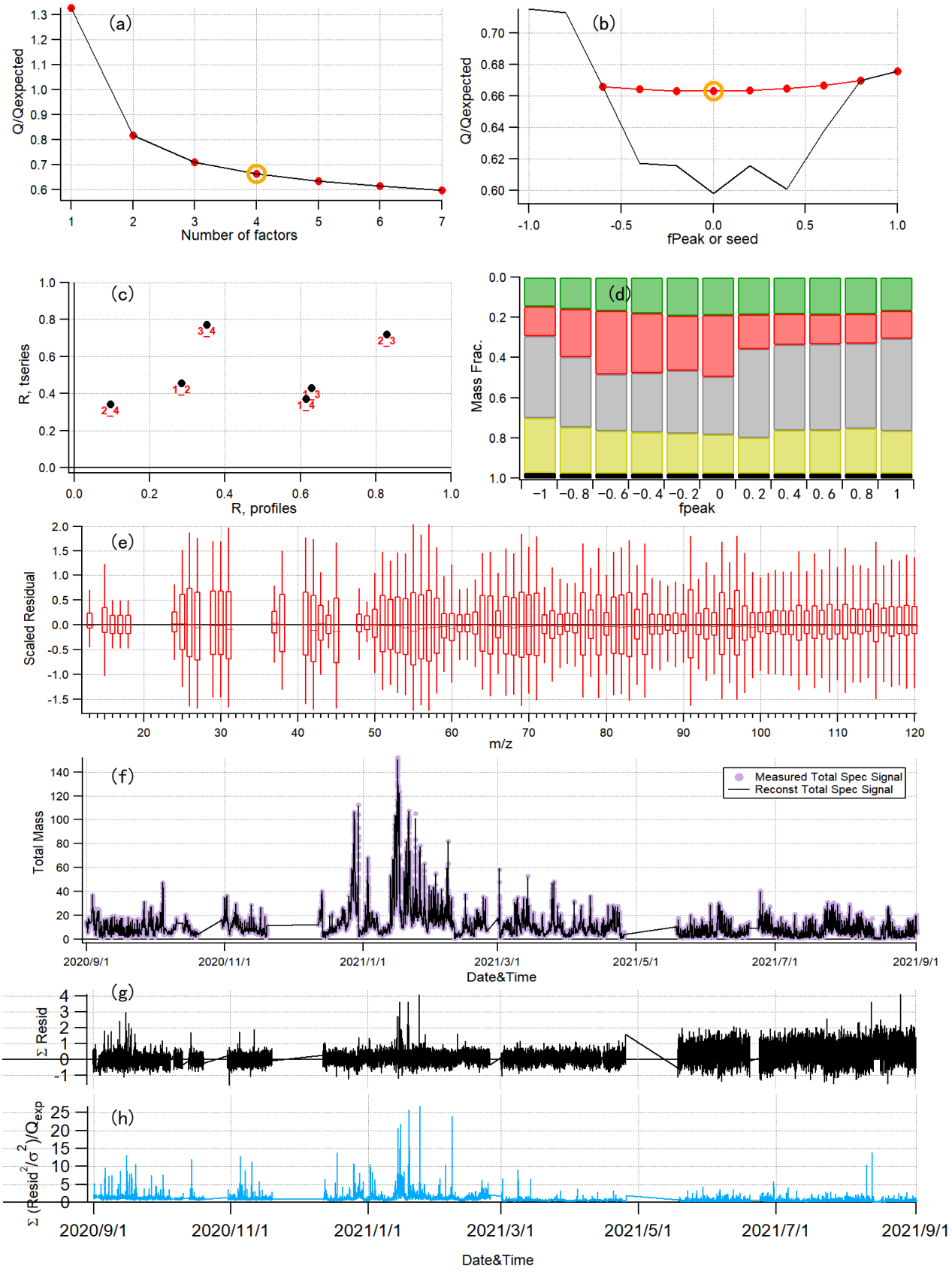

Figure S3. Diagnostic plots of the 4-factor solution in the unconstrained PMF for the entire dataset.

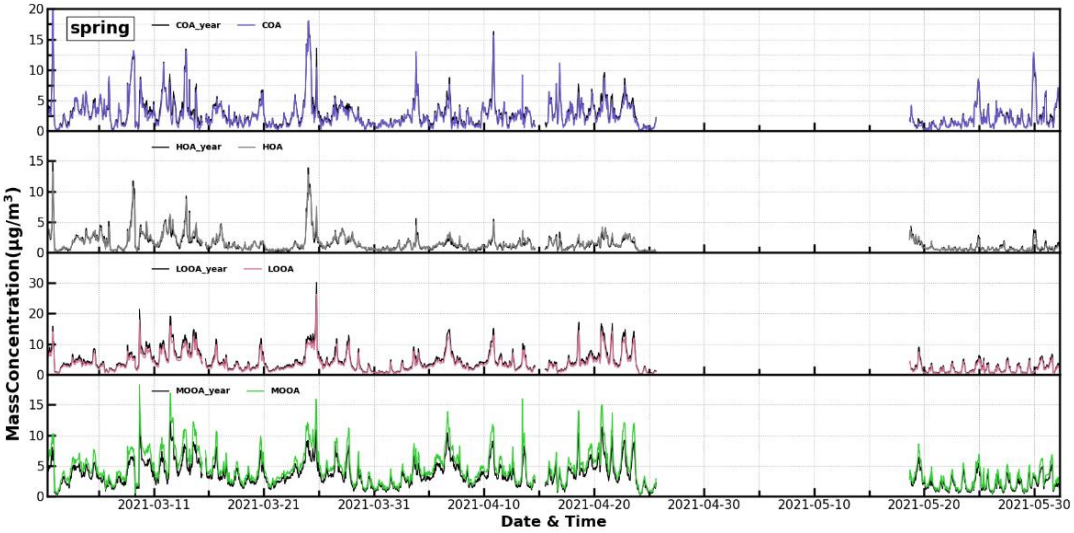

Figure S4. Comparison of time series of ME2-ACSM for the entire dataset in spring and spring dataset.

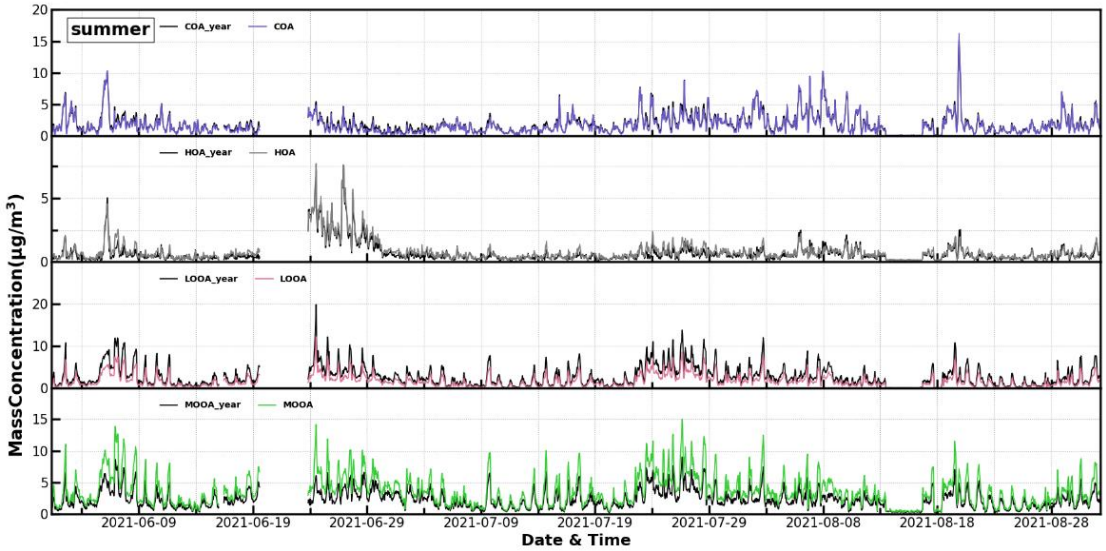

Figure S5. Comparison of time series of ME2-ACSM for the entire dataset in summer and summer dataset.

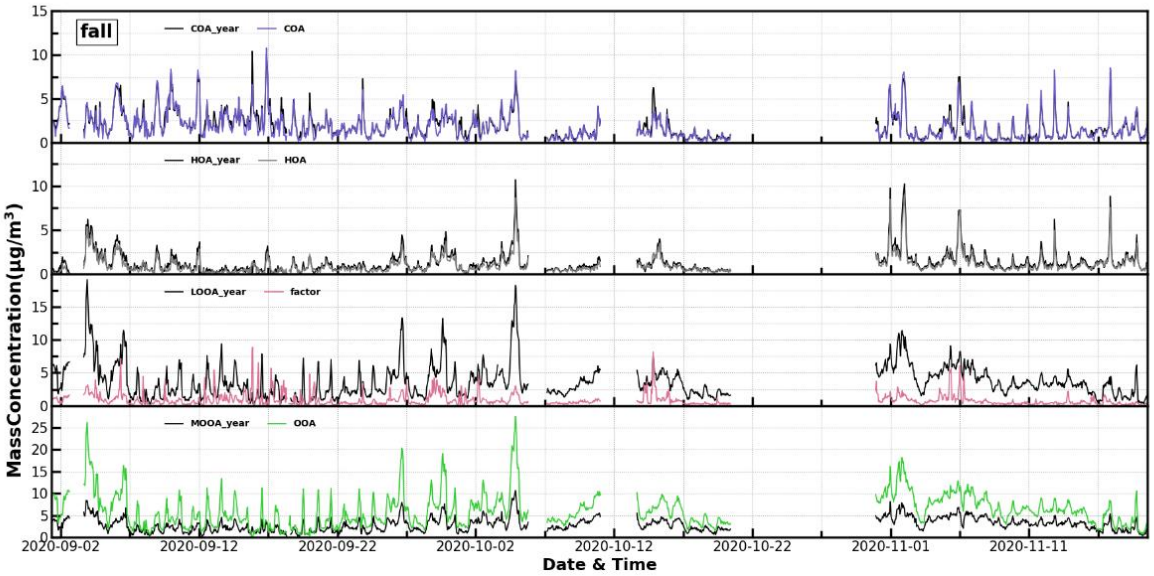

Figure S6. Comparison of time series of ME2-ACSM for the entire dataset in fall and fall dataset.

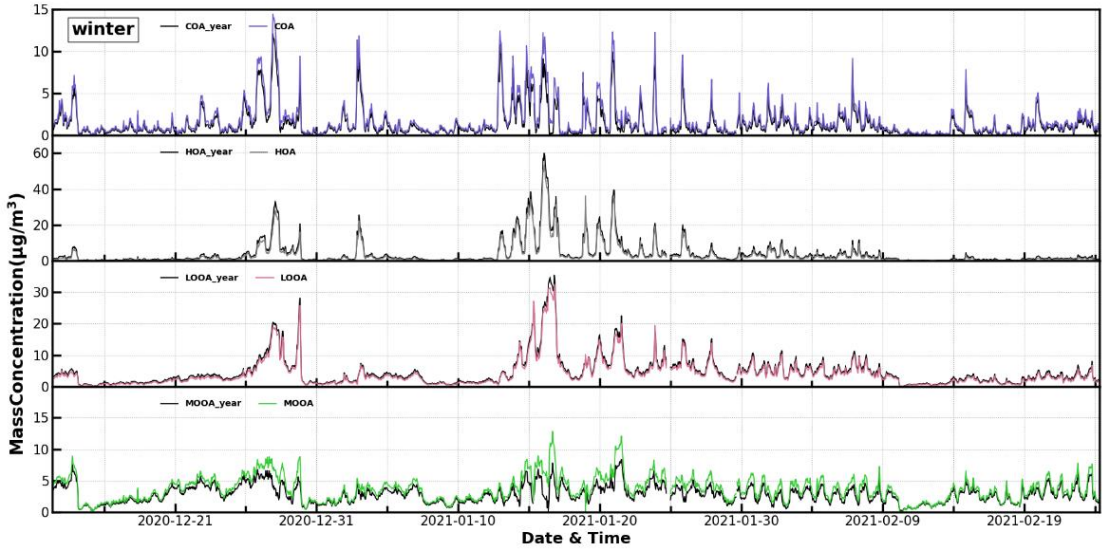

Figure S7. Comparison of time series of ME2-ACSM for the entire dataset in winter and winter dataset.

3. Other supplementary figures

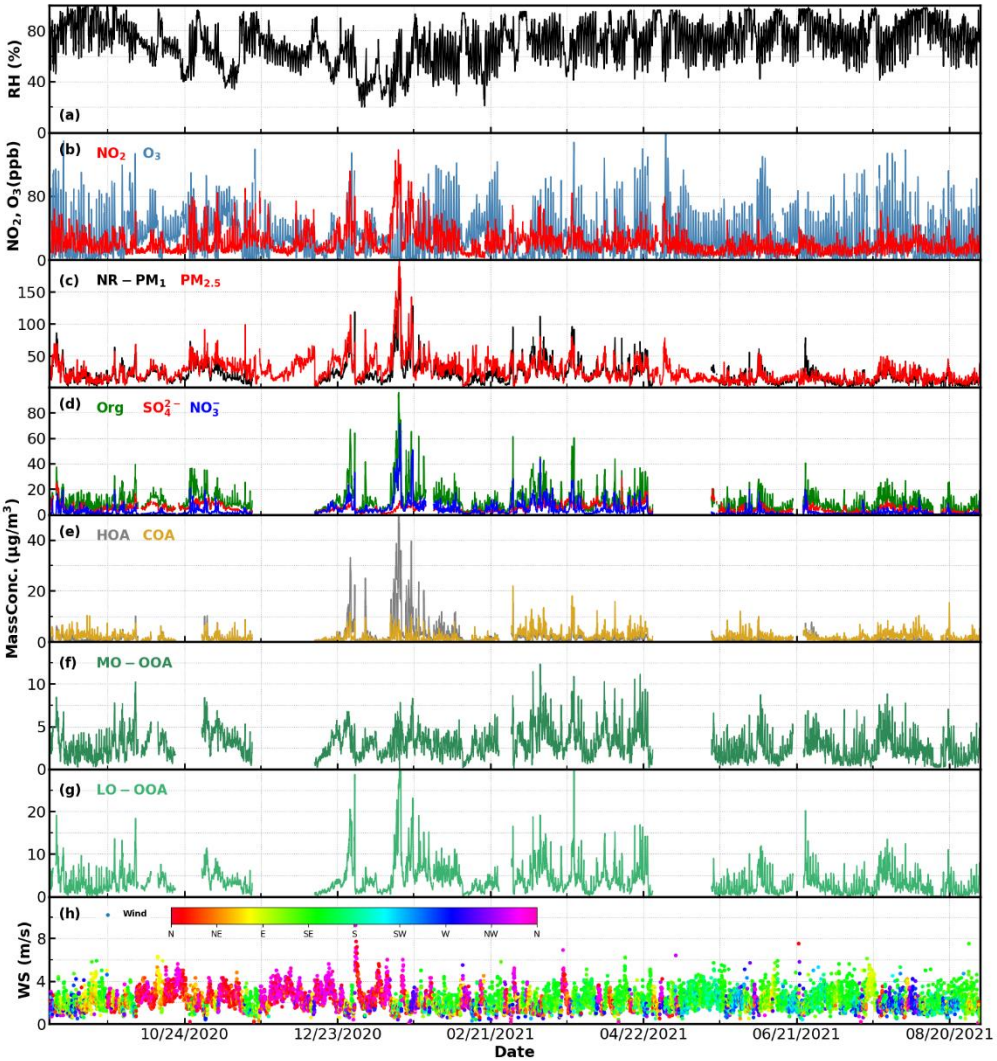

Figure S8. Time series of (a) RH; (b) NO_2 and O_3; hourly average mass concentrations of (c) NR-PM_1 and $PM_{2.5}$; (d) Organics (Org), sulfate (SO_4^{2-}) and nitrate (NO_3^-) and (e-g) four factors from the ME2-ACSM analysis for the entire year, including HOA, COA, MO-OOA and LO-OOA and (h) wind speed (WS) and wind direction (WD).

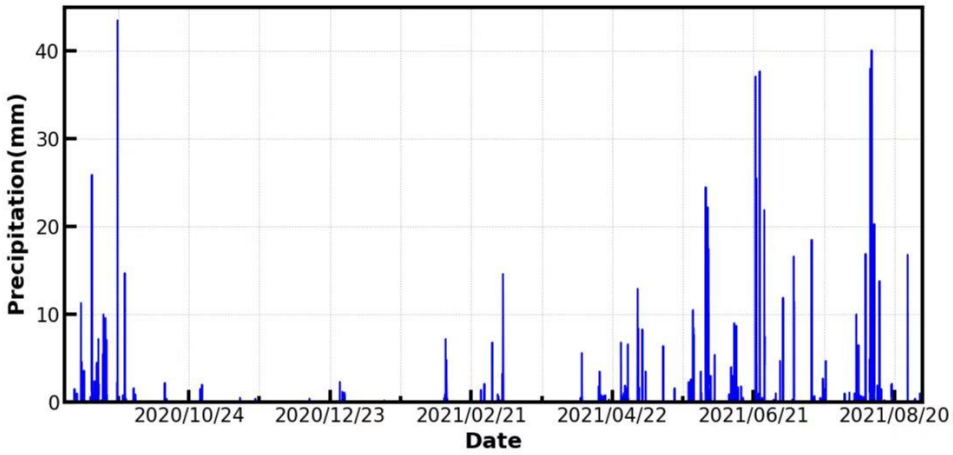

Figure S9. Time series of precipitation during the observations

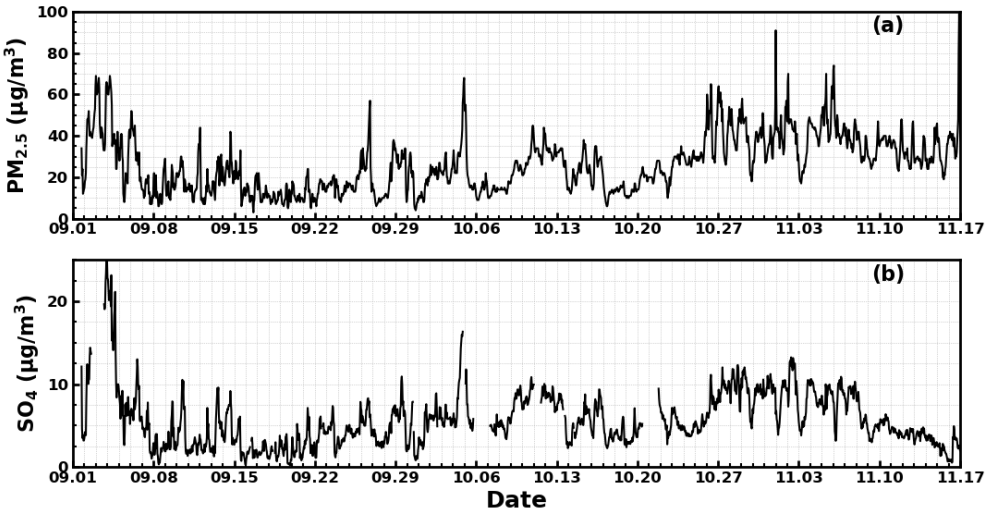

Figure S10. Time series of $PM_{2.5}$ (a) and sulfate (SO_4) (b) during autumn of 2020.

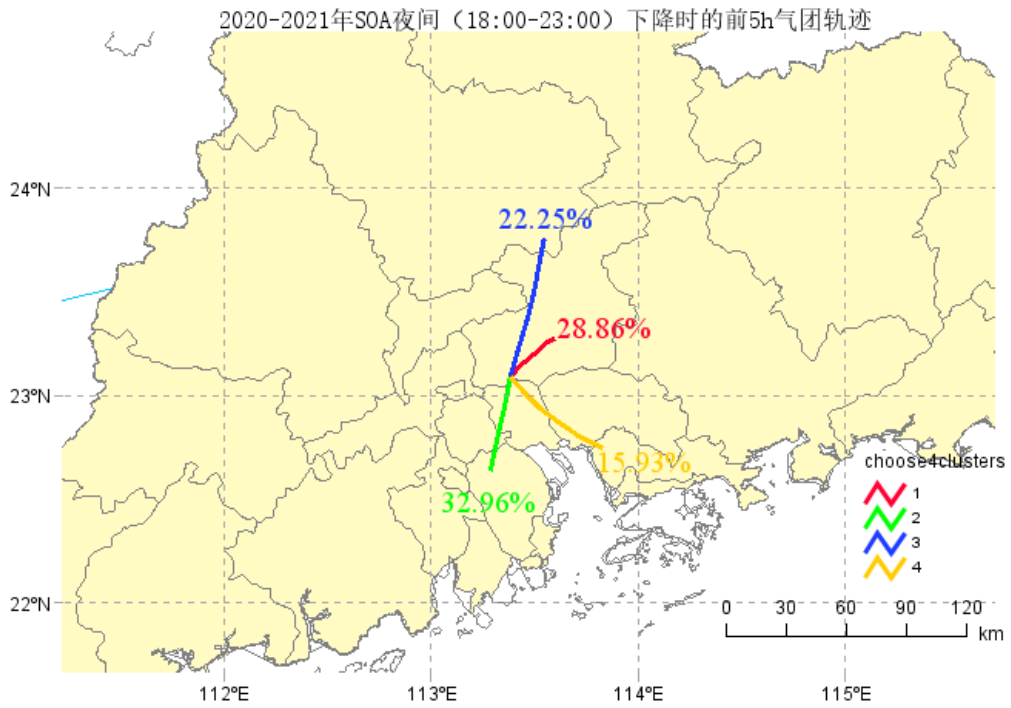

Figure S11. The 5h back trajectories of airflow when SOA decreased at nighttime from 18:00 to 23:00 LT in 2020-2021.

Kuang, Y., Zhao, C. S., Zhao, G., Tao, J. C., Xu, W., Ma, N., and Bian, Y. X.: A novel method for calculating ambient aerosol liquid water content based on measurements of a humidified nephelometer system, Atmospheric Measurement Techniques, 11, 2967-2982, 10.5194/amt-11-2967-2018, 2018.

Liu, L., Kuang, Y., Zhai, M., Xue, B., He, Y., Tao, J., Luo, B., Xu, W., Tao, J., Yin, C., Li, F., Xu, H., Deng, T., Deng, X., Tan, H., and Shao, M.: Strong light scattering of highly oxygenated organic aerosols impacts significantly on visibility degradation, Atmos. Chem. Phys., 22, 7713-7726, 10.5194/acp-22-7713-2022, 2022.